



# Imprint and short-term fate of the Agia Zoni II tanker oil spill on the marine ecosystem of Saronikos Gulf

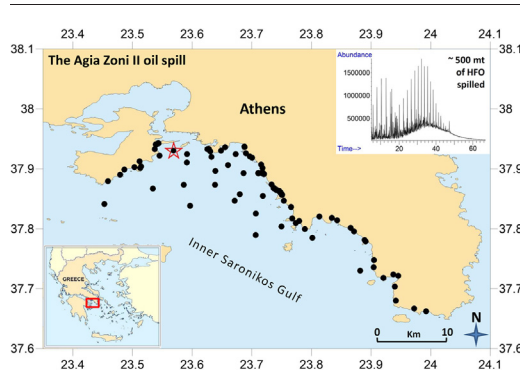
C. Parinos\*, I. Hatzianestis, S. Chourdaki, E. Plakidi, A. Gogou

*Institute of Oceanography, Hellenic Centre for Marine Research (H.C.M.R.), 46.7 Km Athens-Sounio av., Mavro Lithari, 19013 Anavyssos, Attiki, Greece*

## HIGHLIGHTS

- The Agia Zoni II incident released ~500 mt of HFO in the Saronikos gulf, Greece.
- The oil was rapidly beached causing an extended petroleum imprint along-shore.
- High PAH levels were recorded in sea-water the first three months from the spill.
- Sediments were not seriously affected from the spilled oil.
- Volatilization, rapid biodegradation and photodegradation affected the spilled oil.

## GRAPHICAL ABSTRACT



## ARTICLE INFO

### Article history:

Received 12 June 2019

Received in revised form 22 July 2019

Accepted 22 July 2019

Available online 23 July 2019

Editor: Damia Barcelo

### Keywords:

Agia Zoni II

Oil spill

Saronikos Gulf

Heavy fuel oil

## ABSTRACT

In this study we investigate the spatial and temporal imprint of the September 2017 Agia Zoni II tanker heavy fuel oil spill on the marine ecosystem of Saronikos Gulf (Greece). Based on the chemical fingerprinting approach, by means of gas chromatography - flame ionization detector, gas chromatography-mass spectrometry and the use of various diagnostic ratios, we characterize changes in the composition of the spilled oil at various sampling sites and evaluate major mechanisms affecting its fate i.e. dissolution/dispersion, evaporation, biodegradation, photo-oxidation and sedimentation during the first six months from the spill. Overall, the main effects of the incident were confined to the coastal zone during the first three months after the spill, where an extended petroleum imprint was recorded in many cases, with the determined concentrations of the total petroleum hydrocarbons and polycyclic aromatic hydrocarbons falling within the highest range of concentrations previously reported for similar oil spill incidents worldwide. In the first three months following the spill the oil was affected by a combination of volatilization, rapid biodegradation and photodegradation, the later playing a role in its early days weathering. Concerning sediments, an imprint related to the incident was recorded in a few cases, being, however, mild in respect to the high chronic petroleum-associated anthropogenic background of the impacted area.

© 2019 Elsevier B.V. All rights reserved.

## 1. Introduction

On September 10th 2017, the oil/chemical tanker Agia Zoni II sank at anchor, under good weather conditions, outside the northern part of the Piraeus anchorage area in Saronikos Gulf (city of Athens). The vessel was laden with ~ 2194 mt of heavy fuel oil (HFO) and 370 mt of marine

\* Corresponding author at: Hellenic Centre for Marine Research, Institute of Oceanography, Anavyssos, Attiki, Greece.

E-mail address: [ksparinos@hcmr.gr](mailto:ksparinos@hcmr.gr) (C. Parinos).

gas oil (MGO), while the vessel also carried ~ 15 mt of MGO bunkers. It is believed that ~ 500 mt of HFO (group IFO 380) were released upon sinking and shortly thereafter. In the following days the oil stranded along 4 km of shoreline on the Salamina Island as well as 25 km of shoreline on the densely populated and of very high economical value Piraeus/Athens Riviera. Clean-up operations were commenced very shortly after the incident and continued through autumn 2017 gradually concluding before or on December 3rd 2017. On November 29th 2017 the shipwreck was lifted from the seafloor and towed to a nearby shipyard (IOPC, 2019).

The Saronikos Gulf is situated at the west-central Aegean Sea (north-east Mediterranean Sea) surrounded by the peninsulas of Attica to the north and Peloponnese to the southwest, while it communicates with the Aegean Sea to the east. There are several islands and islets in the gulf, with Salamina and Aigina being the most important in terms of size and population density. The length of the coastline is ~270 km, the sea surface covers ~2.866 km<sup>2</sup> and the average water depth is ~100 m. The Agia Zoni II incident occurred at the northern part of the eastern basin (~135 km), called Inner Saronikos Gulf (Fig. 1). From the very first days of the incident (day 8), following the securing of the oil leak from the wreck, a survey network has been set up by the Hellenic Centre for Marine Research (H.C.M.R.) in order to assess the possible short- and medium-term environmental consequences in the impacted areas (H.C.M.R., 2018).

Herein, we examine the spatial and temporal imprint of the spilled oil in the affected areas and characterize changes in its composition at various sampling sites during the first six months from the spill. To

this, we evaluate the major mechanisms affecting its fate i.e. dissolution/dispersion, evaporation, biodegradation, photo-oxidation and sedimentation (NRC, 2003; Tarr et al., 2016) based on the chemical fingerprinting approach by gas chromatography techniques (Wang et al., 2007). The Inner Saronikos Gulf is subjected to intense anthropogenic pressure from several point and nonpoint pollution sources as it constitutes the coastal receptor area of the metropolitan city of Athens with approximately four million inhabitants. Intense marine traffic, industries, oil refineries, marinas, touristic facilities, the industrial zone of Elefsis Bay and Piraeus port (the largest port in Greece and one of the biggest in Europe), affect the marine environment of Saronikos Gulf via runoff and/or submarine groundwater discharges and atmospheric deposition of pollutants from the adjacent urban areas (Kalabokas et al., 2001; Kapsimalis et al., 2014; Panagiotopoulos et al., 2010; Pavlidou et al., 2014; Vasilakos et al., 2007; Xenarios and Bithas, 2009). Considering this, care has been taken in differentiating the incident's imprint from the high chronic petroleum-associated anthropogenic background reported for the study area (Botsou and Hatzianestis, 2012; Hatzianestis et al., 2004; Kapsimalis et al., 2014; Sklivagou et al., 2008).

## 2. Materials and methods

### 2.1. Sampling strategy

In order to evaluate the spatial and temporal distribution of dissolved/dispersed petroleum hydrocarbons in the water column of the

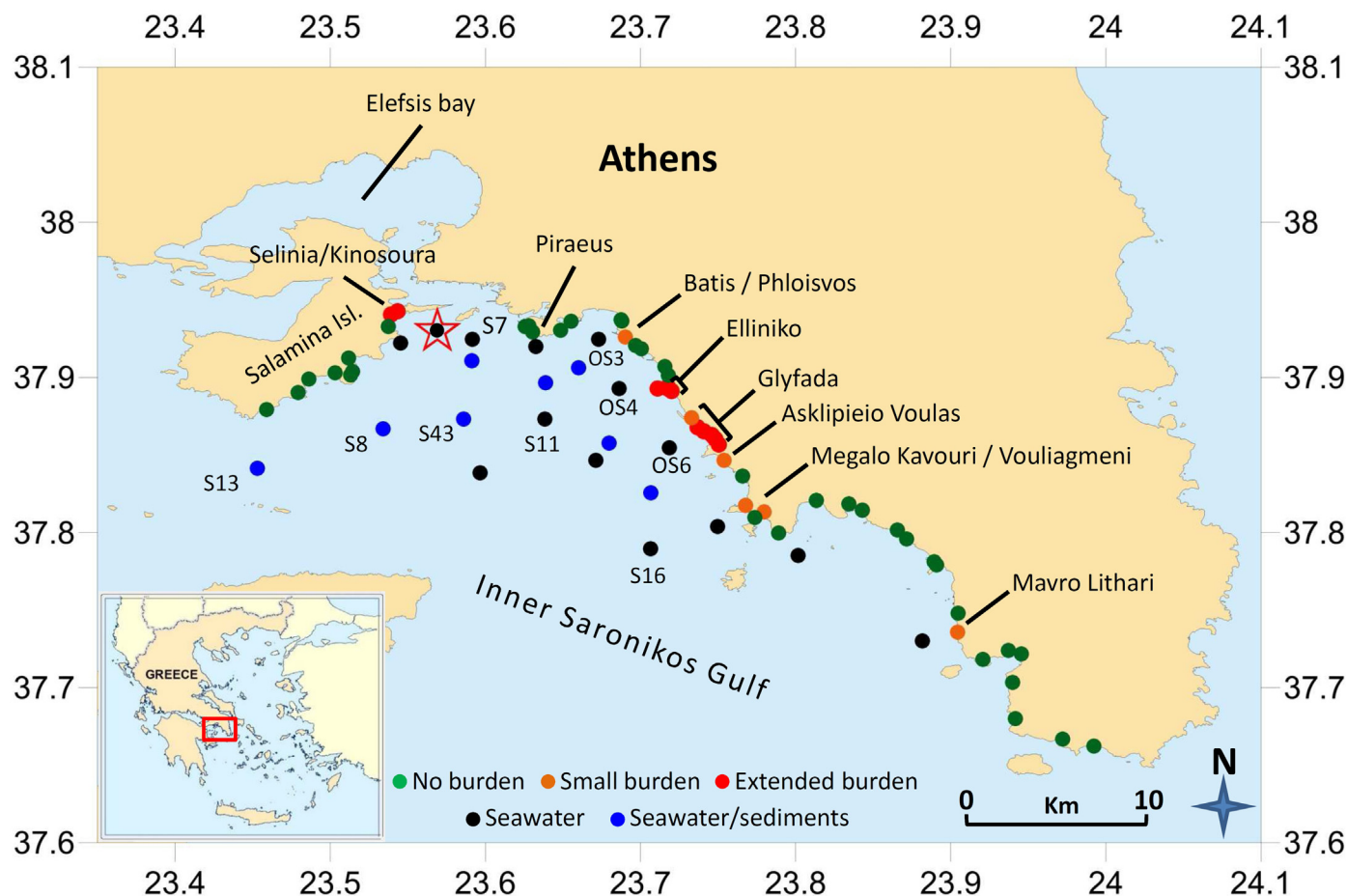


**Fig. 1.** Map of the wider Inner Saronikos Gulf annotated with all major features discussed in the main text. The red star marks the Agia Zoni II tanker sinking position, coastal stations marked green are the ones where TPH concentrations were recorded within background levels at the time of their sampling in all cases, while coastal stations marked red and orange respectively are the areas where an extended or smaller burden of petroleum hydrocarbons was recorded. Seawater sampling positions in open sea sites are marked as black, while sediment sampling positions in open sea sites are marked both in black and blue. (For interpretation of the references to color in this figure legend, the reader is referred to the web version of this article.)

study area, seawater samplings at various sites of the coastal zone of Saronikos Gulf were conducted on September 18th, 22nd, 29th, October 3rd, 10th, 23rd, November 2nd and December 4th 2017, January 19th and March 21st 2018. The water samples (2.5 L volume) were collected by means of a sampling device consisting of a weighted bottle holder with a clean amber-glass bottle and Teflon-lined cap (UNEP, 1984). Moreover, seawater samplings were undertaken on September 21–22nd 2017 and November 13–14th 2017 in open sea sites of Saronikos Gulf from the sea surface and various water depths of the water column. In the vicinity of the Agia Zoni II shipwreck (~60 m from the antipollution barrier) seawater samples were collected from six depths of the water column. All samples were collected with 10 L Niskin bottles mounted on a rosette sampler. In all cases, 2.5 L of seawater were immediately transferred to clean amber-glass bottles with Teflon-lined caps. In total the survey effort included 69 sampling sites, of which 55 coastal within the boundaries of eleven municipalities, and 14 open sea areas, while a total of 247 samples were considered. None of the collected seawater samples was filtrated, thus representing a mixture of hydrocarbons from both the dissolved and particulate phases, while each one of them was preserved with 50 mL of Suprasolv *n*-hexane. All samples were immediately transferred back to the laboratory and were analyzed within two to three days after their collection in all cases. The coastal and open sea sampling sites in the Saronikos Gulf are illustrated in Fig. 1, while detailed sampling positions and sampling dates are depicted in supplementary Tables S.1 and S.2, respectively.

Major weathering mechanisms affecting the composition of the spilled oil were examined in oil patches collected along shore the areas where the main mass of the spill had beached. Samples were collected with a metal spoon, placed in pre-cleaned amber glass jars and were transferred back to the laboratory where they were stored at  $-20^{\circ}\text{C}$  till further analysis. Following the initial days of the spill the occasions of slumps appearing at sea or arriving at the coast were very few in number and limited in amount of appearing individuals. Also, over time patches were very difficult to be traced/recovered since the impacted sites were gradually delivered after the completion of extensive clean-up operations under a strict 'as pre-spill condition' requirement. Herein, a total of 16 samples collected along the rocky shoreline of Glyfada region (Fig. 1), heavily impacted by the spill, are considered, spanning in detail the first 85 days after the incident i.e. till the completion of the clean-up operations.

Sediment samplings in open sea sites of the Saronikos Gulf were conducted on September 21–22nd 2017, November 13–14th 2017 and January 23–24th 2018. Our goal was to investigate any possible accumulation of petroleum hydrocarbons on the seabed of the wider Inner Saronikos Gulf. The survey effort included 22 sampling sites with a total of 57 sediment samples being considered. All sediments (top 1-cm) were collected using a stainless steel Box Corer with a surface area of  $40 \times 40$  cm and were wrapped in pre-combusted aluminum foil and immediately stored at  $-20^{\circ}\text{C}$  till further analysis. The sediment sampling sites at open sea areas of the Saronikos Gulf are presented in Fig. 1, while detailed sampling positions are provided in the supplementary Table S.3. The considered sampling stations S7, S8, S11, S13, S16 and S43 (Fig. 1) belong to the Saronikos Gulf systematic monitoring network for which a time series of data is available covering the past twenty years (H.C.M.R., 2016, 2017). They are therefore a reliable basis for comparing data gathered before and after the oil spill incident. The rest of the sediment sampling stations (named as OS1–OS15; see Table S.3) have been added to the existing monitoring network taking into consideration the spill's migration direction.

## 2.2. Analysis

All seawater samples were analyzed for total petroleum hydrocarbons (TPH) and polycyclic aromatic hydrocarbons (PAHs) by means of gas chromatography. After the addition of perdeuterated internal standards ( $[\text{C}_{25}\text{H}_{50}]n$ -tetracosane for TPH;  $[\text{C}_{10}\text{H}_8]$ naphthalene,  $[\text{C}_{12}\text{H}_{10}]$

acenaphthene,  $[\text{C}_{16}\text{H}_{10}]$ phenanthrene,  $[\text{C}_{16}\text{H}_{12}]$ pyrene,  $[\text{C}_{18}\text{H}_{12}]$ chrysene,  $[\text{C}_{20}\text{H}_{12}]$ perylene and  $[\text{C}_{22}\text{H}_{12}]$ benzo[ghi]perylene for PAHs) the samples were extracted with *n*-hexane within 2–3 days after their collection. *n*-Hexane extracts were dried over sodium sulphate, concentrated by vacuum rotary evaporation and then fractionated on an activated silica gel column in order to remove polar components. Two fractions were collected, the first one with 10 mL of *n*-hexane containing the aliphatic hydrocarbons and the second one with 10 mL of *n*-hexane-ethyl acetate (9:1, v/v) containing the PAHs, which were combined for chromatographic analysis. Combined fractions were concentrated by vacuum rotary evaporation, transferred to 1.5 mL amber vials and excess solvent was evaporated under a gentle nitrogen stream.

TPH were determined by gas chromatography - flame ionization detector (GC/FID) on an Agilent 7890 GC equipped with an HP-5MS capillary column ( $30 \text{ m} \times 0.25 \text{ mm i.d.} \times 0.25 \mu\text{m}$  phase film). PAHs determination was performed by gas chromatography-mass spectrometry (GC/MS) on an Agilent 7890 GC, equipped with an HP-5MS capillary column ( $30 \text{ m} \times 0.25 \text{ mm i.d.} \times 0.25 \mu\text{m}$  phase film), coupled to an Agilent 5975C MSD using a selected ion monitoring (SIM) acquisition program. Details regarding the instrumental analysis parameters are described elsewhere (Botsou and Hatzianestis, 2012; Parinos et al., 2013a).

TPH were estimated by integrating the areas of the resolved and unresolved aliphatic components using the baseline corrected total area of the chromatogram and the average *n*-alkanes response factor determined over the entire analytical range ( $n\text{-C}_{10}$  to  $n\text{-C}_{40}$ ) (Douglas et al., 1992). In the case of PAHs the quantified compounds included the parent compounds with molecular weights ranging from 128 to 278, and the methylated derivatives of naphthalene, dibenzothiophene, phenanthrene, pyrene and chrysene, being 32 compounds/groups in total (referred to hereafter as  $\Sigma\text{PAH}_{32}$ ). Standard solutions of the targeted PAH compounds, purchased from Dr. Ehrenstorfer GmbH, were spiked with the internal standards and run on each injection set in order to derive relative response factors (RRFs) of the analytes. The precision of the analytical method, evaluated in terms of repeatability of the experimental results ( $n = 7$ ; in spiked samples) and expressed in terms of relative standard deviation, was 4.6% for TPH and ranged from 1.8 to 5.1% for individual PAHs. Procedural blanks were found to be free of any interference. The organic chemistry laboratory of H.C.M.R. is accredited by ISO/IEC 17025 for the analysis of PAHs in marine waters.

Concerning the recovered sediments, all samples were initially freeze-dried and subsequently homogenized. For the analytical determination of hydrocarbons, 5 g of sediment were spiked with a mixture of perdeuterated internal standards ( $[\text{C}_{25}\text{H}_{50}]n$ -tetracosane for aliphatic hydrocarbons;  $[\text{C}_{10}\text{H}_8]$ naphthalene,  $[\text{C}_{12}\text{H}_{10}]$ acenaphthene,  $[\text{C}_{16}\text{H}_{10}]$ phenanthrene,  $[\text{C}_{16}\text{H}_{12}]$ pyrene,  $[\text{C}_{18}\text{H}_{12}]$ chrysene,  $[\text{C}_{20}\text{H}_{12}]$ perylene and  $[\text{C}_{22}\text{H}_{12}]$ benzo[ghi]perylene for PAHs) and then extracted into a Soxhlet apparatus for 24 h with a methanol-dichloromethane mixture (1:2, v/v). Subsequently, the extract was saponified with a methanolic potassium hydroxide solution and the non-saponified components were extracted with *n*-hexane. The extract was then fractionated on an activated silica gel column and two fractions were collected, the first one with 10 mL of *n*-hexane containing the aliphatic hydrocarbons and the second one with 10 mL of *n*-hexane-ethyl acetate (9:1, v/v) containing the PAHs. Both fractions were concentrated by vacuum rotary evaporation, transferred to a 1.5 mL amber vial and excess solvent was evaporated under a gentle nitrogen stream. The final determination of aliphatic and polycyclic aromatic hydrocarbons was performed by GC/MS on an Agilent 7890 GC, equipped with an HP-5MS capillary column ( $30 \text{ m} \times 0.25 \text{ mm i.d.} \times 0.25 \mu\text{m}$  phase film), coupled to an Agilent 5975C MSD as described elsewhere (Botsou and Hatzianestis, 2012; Kapsimalis et al., 2014).

The quantified compounds were *n*-alkanes ranging from  $n\text{-C}_{14}$  to  $n\text{-C}_{36}$ , along with the isoprenoids pristane (Pri) and phytane (Phy), the unresolved complex mixture (UCM) and the total amount of the resolved aliphatic compounds (RC), and  $\Sigma\text{PAH}_{32}$  as defined above.



Results are reported per dry weight of sediment in all cases. The accuracy of PAHs determination was evaluated by analyzing the National Institute of Standards reference sediment SRM 1941b - NIST USA (organics in marine sediment). The determined values ranged between 92.4 and 108.3% of the certified values. Standard solutions of the targeted PAH compounds, purchased from Dr. Ehrenstorfer GmbH, were spiked with the internal standards and run on each injection set in order to derive relative response factors (RRFs) of the analytes. The precision in the analysis of the samples, evaluated in terms of repeatability of the experimental results ( $n = 7$ ) and expressed in terms of relative standard deviation, was 5.2% for the UCM and total RC and ranged from 1.4 to 5.9 and 4.1 to 9.1% for PAHs and  $n$ -alkanes, respectively. Procedural blanks processed were found to be free of contamination. The organic chemistry laboratory of H.C.M.R. is accredited by ISO/IEC 17025 for the analysis of PAHs in marine sediments.

Regarding the oil patches, the collected samples were dissolved in dichloromethane and stored in amber glass vials with Teflon-lined caps till further analysis. For the analytical determination of hydrocarbons the same procedure as in the case of sediments was followed concerning internal standards addition, fractionation and final GC/MS analysis.

### 3. Results and discussion

#### 3.1. Source oil characterization

In order to discriminate the imprint caused by the oil spill incident from the chronic petroleum-associated anthropogenic background of the wider Inner Saronikos Gulf area a source oil sample drawn from the wreck on September 16th 2017 has also been considered as a reference. A GC trace of the aliphatic fraction of the Agia Zoni II source oil is presented in Fig. 2a. It is characterized by an  $n$ -alkane range from  $n$ -C<sub>10</sub> to  $n$ -C<sub>36</sub> and a bimodal distribution with the first mode centered at  $n$ -C<sub>11</sub> and the second one at  $n$ -C<sub>22</sub>. This distribution is consistent to the dilution of the HFO with a lighter distillate/cutting oil (such as light diesel) (Wang et al., 1999). The Pri/Phy ratio was 0.87. Regarding PAHs, the source oil is characterized by a high percentage of naphthalene and its alkylated homologues (~40% of the total determined PAHs) followed by the phenanthrene series (~25%), dibenzothiophene series (~9%) and pyrene and chrysene series comprising ~10% and ~8.5% of the determined PAH compounds respectively (Fig. 2b), presumably originating from the lighter blending oil (Uhler et al., 2007). Within the determined PAH series the proportion of the alkylated homologues in relation to the parent compounds follows the order  $C_0 < C_1 < C_2 > C_3$  in all cases. The Agia Zoni II oil also contained traces of 5- and 6-ring PAH compounds being <0.3% of the  $\Sigma$ PAH<sub>32</sub> in all cases (Fig. 2b). 2-Methyl anthracene (2MA), a PAH not frequently found in crude oils (Uhler et al., 2007), was determined in the source oil, however, the concentrations of terpanes ( $m/z$  191) were very low, while steranes ( $m/z$  217) were practically absent.

#### 3.2. Spatial/temporal distribution of dissolved/dispersed petroleum hydrocarbons

The results from the determination of TPH and  $\Sigma$ PAH<sub>32</sub> concentrations in the seawater samples collected from the coastal zone and open sea sites of Saronikos Gulf are summarized in Tables S.1 and S.2, respectively.

Regarding the open sea sampling sites, at both conducted samplings TPH concentrations were low, ranging in all cases from not detected to <20  $\mu\text{g L}^{-1}$  a background value that has often been reported for the inner Saronikos Gulf waters according to available data spanning the last decade (Hatzianestis, unpublished data; 98 observations). In the September 2017 sampling (11 days after the incident) the TPH concentrations ranged from not detected to 6.8  $\mu\text{g L}^{-1}$  while in the November 2017 sampling (64 days after the incident) the TPH concentrations

ranged from not detected to 3.9  $\mu\text{g L}^{-1}$ . Likewise,  $\Sigma$ PAH<sub>32</sub> concentrations fluctuated at low levels, i.e. between 8.23 and 125  $\text{ng L}^{-1}$  at both samplings, in accordance to those previously reported for the study area and Greek seas (Hatzianestis and Sklivagou, 2002; Parinos and Gogou, 2016). The above are indicative of the rapid transport of the spilled oil to the coastal zone in the very first days after the incident, driven by the prevailing winds across the Saronikos Gulf area during that period, i.e. 5–6 on the Beaufort scale, initially on a E/SE and later on a W/SW direction (data available at <http://meteosearch.meteo.gr/data/alimos/2017-09.txt> operated by Institute for Environmental Research and Sustainable Development of the National Observatory of Athens) (Lagouvardos et al., 2017).

Indeed, an extended petroleum imprint, in many cases >1500  $\mu\text{g L}^{-1}$  and up to 3080  $\mu\text{g L}^{-1}$  for TPH concentrations (Table S.1), was recorded as early as 8 days and on from the incident in Selinia and Kynosoura at Salamina Island and along the shorelines of the Elliniko and Glyfada regions (see Fig. 1 sampling stations marked as red) where the main mass of the spill had beached (Fig. S1). In these cases  $\Sigma$ PAH<sub>32</sub> reached values as high as 62.6  $\mu\text{g L}^{-1}$ . Moreover, and despite their low water solubility, concentration values for the toxic benzo[a]pyrene and benzo[ghi]perylene (Boehm and Page, 2007; Neff, 2002) high above the maximum allowable threshold (MAC) according to EU environmental quality standards for the determination of chemical and ecological status of waters (EC, 2013) were recorded, i.e. up to 155  $\text{ng L}^{-1}$  for benzo[a]pyrene (MAC being 27  $\text{ng L}^{-1}$ ) and up to 22.6  $\text{ng L}^{-1}$  for benzo[ghi]perylene (MAC being 0.82  $\text{ng L}^{-1}$ ). The TPH and PAHs values reported in this study fall within the highest range of concentrations previously reported for similar oil spill incidents worldwide (González et al., 2006; Guitart et al., 2008; Kennicutt et al., 1991; Reddy and Quinn, 2001). It should be considered however that the heavy nature of the spilled oil makes it likely to partition into non-aqueous phases. Thus, the reported results for these abovementioned heavily impacted areas might be overestimated, since the seawater samples were not filtered and could be potentially influenced from particles and/or resuspended sediments bearing a burden from the oil spill. Following the intensification of clean-up operations the TPH and  $\Sigma$ PAH<sub>32</sub> concentrations diminished to background levels on November 2nd 2017 in the Elliniko and Glyfada regions and lastly on December 4th 2017 in Selinia and Kinousoura at Salamina Island (Table S.1).

A smaller imprint of petroleum hydrocarbons associated with the incident was also recorded in some cases, i.e. the coastal area of Phloisvos (till 30 days after the incident), Asklepieio Voulas (till 12 days after the incident), and Megalo Kavouri, Vouliagmeni beach club and Mavro Lithari at Anavyssos on day 8 from the incident (see Fig. 1 sampling stations marked as orange). Therein TPH concentrations up to 139  $\mu\text{g L}^{-1}$  and corresponding  $\Sigma$ PAH<sub>32</sub> levels up to 3460  $\text{ng L}^{-1}$  were recorded, which, however, rapidly declined to background levels (Table S.1). In contrast, in the rest 37 out of the 55 considered coastal sites the TPH and  $\Sigma$ PAH<sub>32</sub> concentrations were low, at the time of their sampling, ranging in all cases within background levels i.e. <20  $\mu\text{g L}^{-1}$  for the TPH, with the corresponding concentrations for  $\Sigma$ PAH<sub>32</sub> ranging from 5.34 to 640  $\text{ng L}^{-1}$  (see Fig. 1 sampling stations marked as green).

Following the completion of the clean-up operations, Alimos, Elliniko and Glyfada coastal sites were sampled again in the following winter/early spring months after severe weather events (dominant W/SW winds) followed by rough sea, i.e. on January 19th (up to 9 on the Beaufort scale the previous days) and March 21st 2018 (up to 7 on the Beaufort scale the previous days). This aimed to monitor any transport of oil possibly accumulated near shore and/or the washout of/if any potentially trapped oil especially in rocky coasts. Out of the 13 sampling sites considered only in two cases a slight imprint of petroleum hydrocarbons linked to the incident was recorded, i.e. at Batis and Aigyptiotes Naval Club in Elliniko (Fig. 1) on January 19th 2018, with the TPH concentrations being 45.4  $\mu\text{g L}^{-1}$  (1700  $\text{ng L}^{-1}$  for  $\Sigma$ PAH<sub>32</sub>) and 34.9  $\mu\text{g L}^{-1}$  (697  $\text{ng L}^{-1}$  for  $\Sigma$ PAH<sub>32</sub>) respectively (Table S.1).

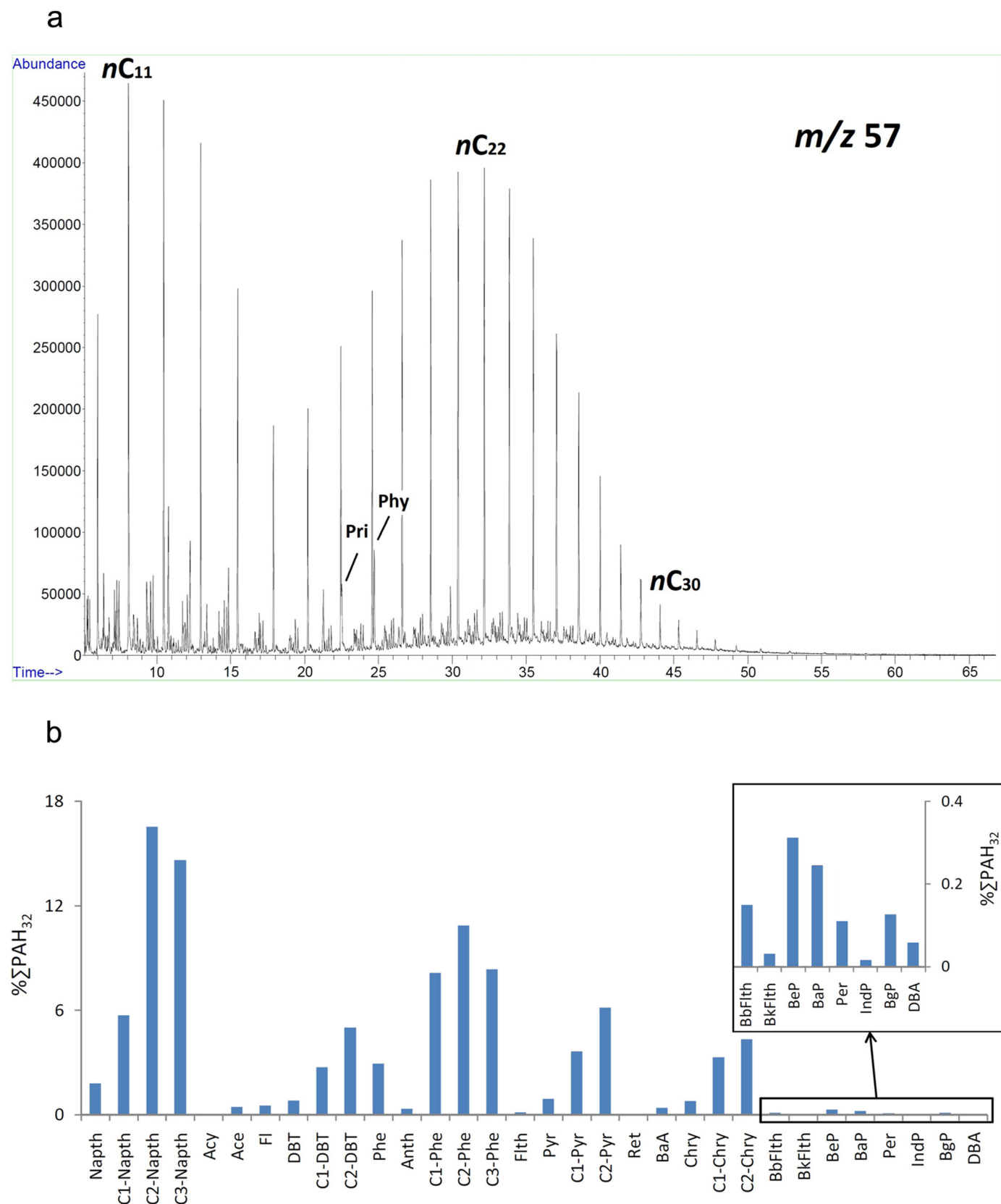
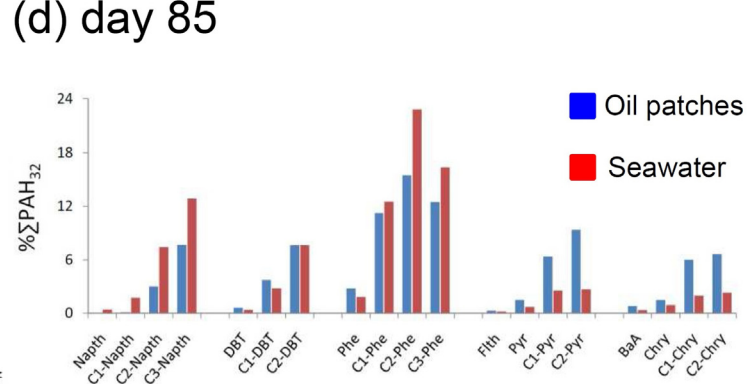
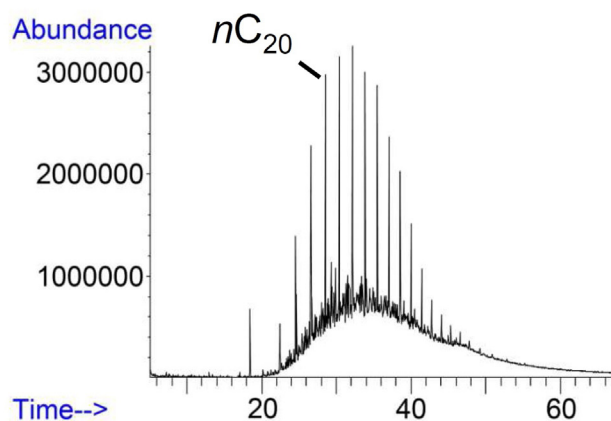
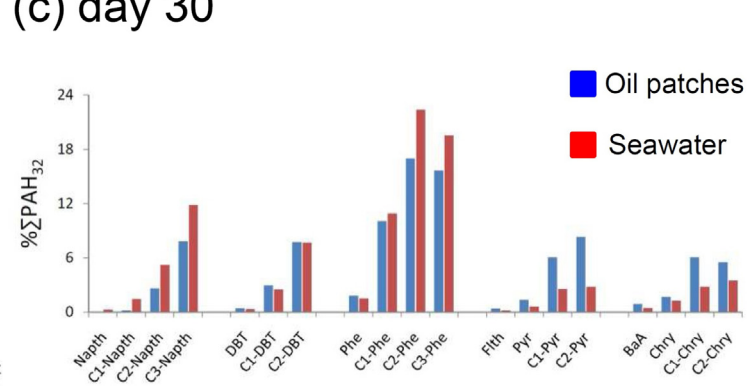
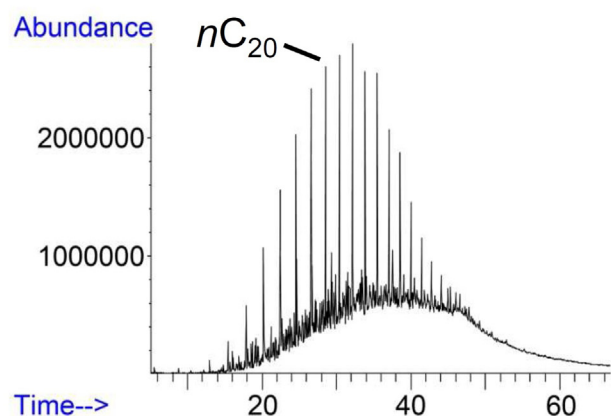
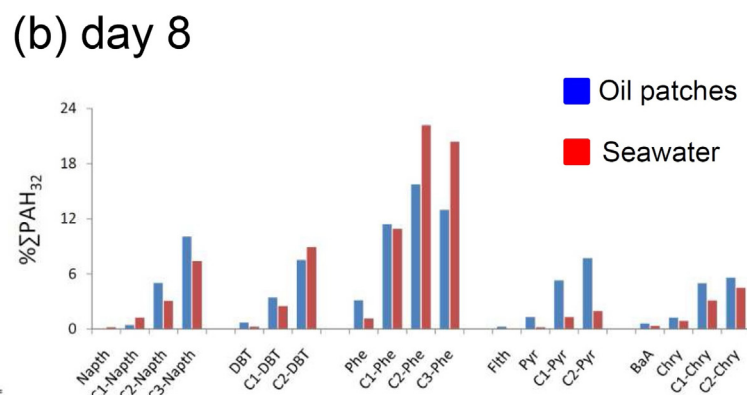
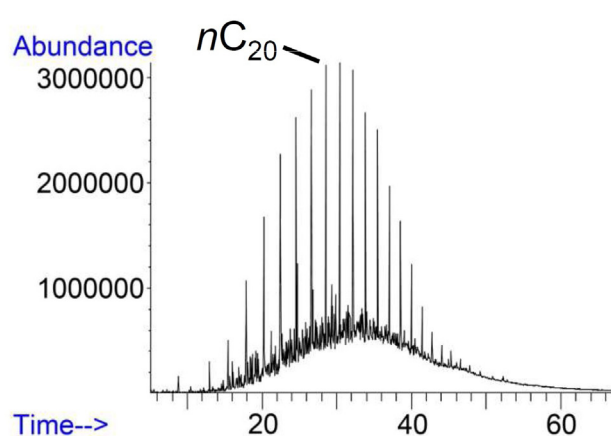
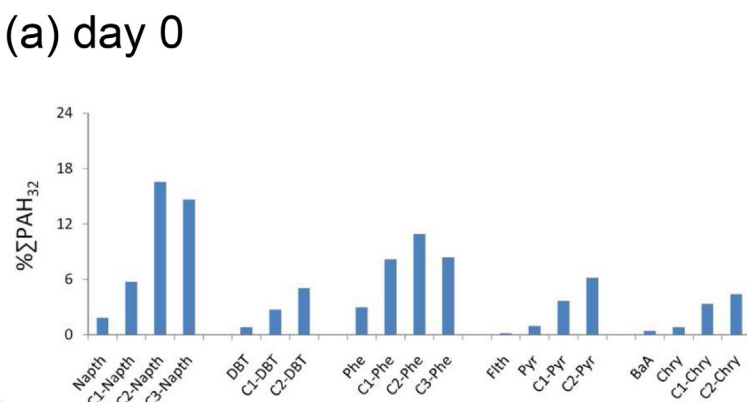
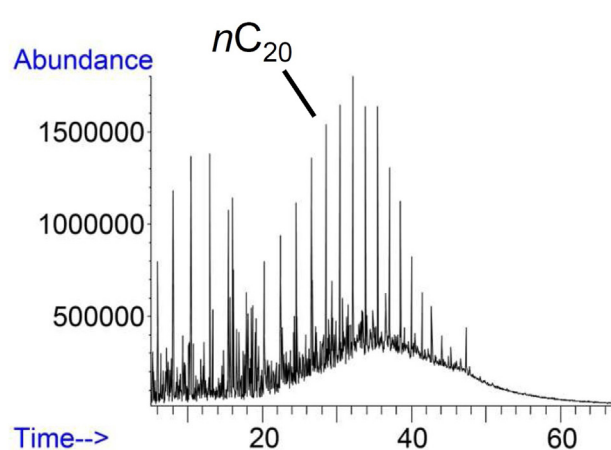


**Fig. 2.** GC/MS ion chromatogram profile ( $m/z$  57) for the aliphatic hydrocarbons (A) and profile of PAHs (B) in the Agia Zoni II reference oil sample. Pri: pristane, Phy: phytane, PAH abbreviations are: naphthalene (Naph); methyl naphthalenes ( $C_1$ -Naph); dimethyl naphthalenes ( $C_2$ -Naph); trimethyl naphthalenes ( $C_3$ -Naph); acenaphthylene (Acy); acenaphthene (Ace); fluorene (Fl); dibenzothiophene (DBT); methyl dibenzothiophenes ( $C_1$ -DBT); dimethyl dibenzothiophenes ( $C_2$ -DBT); phenanthrene (Phe); anthracene (Anth); methyl phenanthrenes ( $C_1$ -Phe); dimethyl phenanthrenes ( $C_2$ -Phe); trimethyl phenanthrenes ( $C_3$ -Phe); fluoranthene (Flth); pyrene (Pyr); methyl pyrenes ( $C_1$ -Pyr); dimethyl pyrenes ( $C_2$ -Pyr); retene (Ret); benz[a]anthracene (BaA); chrysene/triphenylene (Chry); methyl chrysenes ( $C_1$ -Chry); dimethyl chrysenes ( $C_2$ -Chry); benzo[b]fluoranthene (BbFlth); benzo[k]fluoranthene (BkFlth); benzo[e]pyrene (BeP); benzo[a]pyrene (BaP); perylene (Per); indeno[1,2,3-cd]pyrene (IndP); benzo[ghi]perylene (BgP) and dibenz[a,h]anthracene (DBA).



### 3.3. Changes in the composition of the spilled oil

From the early days of the spill event (day 8), a decrease of the *n*-alkanes in the  $<n-C_{20}$  range was observed in the aliphatic fraction of the collected oil patches, being indicative of the rapid loss of light hydrocarbons due to evaporation (Fig. 3b). The loss of low molecular weight hydrocarbons by evaporation is considered as the dominant weathering process in the first days following an oil spill (Gros et al., 2014a; Stout and Wang, 2007) owed to their high vapor pressure (Lemmon and Goodwin, 2000). Moreover, within the aromatic fraction of the considered oil patches the most prominent change was the rapid decrease of the relative abundance of naphthalene and its alkylated derivatives (from ~40% of the  $\sum PAH_{32}$  in the source oil to ~15% of the sum of determined PAHs), with respect to higher ring PAH compounds, in an order of  $C_0 < C_1 < C_2 < C_3$  as the degree of alkylation increases within the series (day 8; see Fig. 3b) being consistent with what anticipated for evaporation and/or dissolution. Evaporation and dissolution are competitive processes acting on similar low molecular weight PAH compounds (Díez et al., 2007; Lemkau et al., 2010) and thus their combined effect should be considered with caution. However, in the corresponding PAH profiles of seawater samples collected during the same period (Fig. 3b) a low relative abundance of naphthalene and its alkyl homologues was also noticed, likely indicating evaporation as the dominant weathering process for these compounds. During this time (Sept. 10–18th 2017) ambient temperature in the city of Athens ranged between a low of 23 °C at night to a high of 32 °C in mid-day (data available at <http://meteosearch.meteo.gr/data/alimos/2017-09.txt>) likely favoring the weathering of the spilled oil through evaporation.

The ratios of *n*-C<sub>17</sub> and *n*-C<sub>18</sub> alkanes with respect to the branched isoprenoids pristane and phytane (*n*-C<sub>17</sub>/pristane and *n*-C<sub>18</sub>/phytane) can provide information on the early effect of microbial degradation on *n*-alkanes (Peters et al., 2005; Wang et al., 1999). In the considered samples, the observed decrease in both ratios from the first days of the incident (day 8; see Table 1) indicates the early onset of biodegradation of the spilled oil and overall denotes biological activity over the first 85 days from the spill. Supportive to the above, the relative amount of the chromatographically unresolved compounds increases during the first months from the spill (Table 1), being indicative of the microbial degradation of aliphatic compounds (Wang et al., 1999). Indeed, by day 85 *n*-alkanes in the  $<n-C_{16}$  range were lost while the distribution of heavier compounds, up to *n*-C<sub>36</sub>, over the aforementioned period remained almost unchanged (Fig. 3d) indicating that they were resistant to weathering. The ratios of phenanthrene (medium-low biodegradability) to BaP (very low biodegradability) and phenanthrene to its alkyl-derivatives (the latter being more recalcitrant) have been proposed as biodegradation indicators (Esquinas et al., 2017). In our samples a decrease for both ratios was observed over the studied period, which is similar to the reduction of the diagnostic ratios described above for the aliphatic fraction (Table 1) being indicative of biodegradation, although dissolution processes acting on phenanthrene cannot be excluded (Esquinas et al., 2017; Gros et al., 2014b).

To further elaborate on this we considered proposed weathering diagnostic ratios related to the methyl and dimethyl derivatives of phenanthrene, i.e. MPR (methyl phenanthrene ratio) defined as:  $(3-C_1Phe + 2-C_1Phe)/(9-4-C_1Phe + 1-C_1Phe)$  and DMPR (dimethyl phenanthrene ratio) defined as:  $(3,5- + 2,6- + 2,7-C_2Phe)/(1,3- + 3,9- + 2,10- + 3,10- + 1,6- + 2,9- + 2,5-C_2Phe)$  (Esquinas et al., 2017). In our samples a decrease for MPR ratio was observed over the studied period, being similar to the one described above for the diagnostic ratios of saturates (Table 1), suggesting modifications in the proportion of mono-methylated phenanthrene isomers as a result of weathering

**Table 1**

Diagnostic ratios values evolution, obtained by averaging results of the corresponding considered oil patches, used for elaborating biodegradation and photodegradation as weathering mechanisms affecting the short-term fate of the spilled oil during the first 85 days from the incident. Abbreviations are defined in the text and the legend of Fig. 2.

|   | Day 0 (source oil) | Day 8 | Day 30 | Day 85 |
|---|--------------------|-------|--------|--------|
| No. of collected samples                        |                    | 8     | 5      | 3      |
| Biodegradation                                  |                    |       |        |        |
| <i>n</i> -C <sub>17</sub> /Pri                  | 2.69               | 2.29  | 2.38   | 1.65   |
| <i>n</i> -C <sub>18</sub> /Phy                  | 1.70               | 1.57  | 1.53   | 1.10   |
| UCM/RC  | 2.61               | 4.08  | 5.87   | 5.84   |
| Phe/BaP   | 12.0               | 10.2  | 3.82   | 3.48   |
| Phe/(C <sub>1</sub> -Phe + C <sub>2</sub> -Phe) | 0.16               | 0.12  | 0.07   | 0.05   |
| MPR   | 1.70               | 1.57  | 1.58   | 1.51   |
| DMPR  | 0.19               | 0.20  | 0.21   | 0.19   |
| Photodegradation                                |                    |       |        |        |
| 2MA/1-C <sub>1</sub> Phe                        | 0.45               | 0.19  | 0.21   | 0.20   |
| C <sub>2</sub> -Chry/C <sub>2</sub> -Pyr        | 0.71               | 0.73  | 0.66   | 0.76   |
| BeP/BaP   | 0.79               | 0.63  | 0.67   | 0.63   |
| BaA/Chry  | 0.51               | 0.50  | 0.54   | 0.48   |

which could be attributed to both biodegradation and photodegradation (Esquinas et al., 2017; Radović et al., 2014). However, the DMPR ratio remained rather constant over the first 3 months from the spill (Table 1), most probably following the general biodegradation pattern of the aromatic hydrocarbons where biodegradation decreases with the increase of alkylation (Atlas, 1981). This probably suggests biodegradation rather than photodegradation as the dominant weathering process amongst the phenanthrene series.

In similar HFO spill cases a lag of several weeks before biodegradation was detectable has been reported e.g., the similar in type and amount of spilled oil Cosco Busan (Lemkau et al., 2010), the Bouchard 120 (Arey et al., 2007), but also the Prestige case, although more extensive regarding the amount of spilled oil (Díez et al., 2007). These differences could be attributed to variations in local environments (Atlas, 1981). However, it should also be considered that in the Agia Zoni II case the spilled oil was rapidly beached, thus experiencing a short weathering history offshore, but also the fact that ~75% of its total determined PAHs refers to light compounds and their alkylated homologues which are readily available to biodegradation.

Finally, the potential effect of photodegradation on the weathering of aromatic compounds was examined using ratios of parent and alkyl-substituted PAHs which photodegrade at different rates while are weathered similarly by other processes, i.e. 2MA/1-C<sub>1</sub>Phe, C<sub>2</sub>-Chry/C<sub>2</sub>-Pyr, BaP/BeP, BaA/Chry (Bernabeu et al., 2013; Esquinas et al., 2017; Lemkau et al., 2010; Plata et al., 2008; Radović et al., 2014). In the considered samples the C<sub>2</sub>-Chry/C<sub>2</sub>-Pyr, and BaA/Chry ratios did not exhibit any noticeable temporal trend, however, a decrease of the 2MA/1-C<sub>1</sub>Phe and BaP/BeP ratio values was evident in the early days after the oil spill with both ratios remaining constant during the following months (Table 1). This indicates that although photodegradation might have played a role in the early days weathering of the oil, most likely attributed to the warm sunny weather during this period (Sept. 10–18th 2017), it was not dominant the following months.

### 3.4. Accumulation of petroleum compounds in sediments

Concerning the sediment samples collected in open sea sites of the study area, macroscopically no large sized tar aggregates or traces of extensive petroleum pollution were observed at the time of their sampling either in the surface or sub-surface layers. The results of the

**Fig. 3.** (Left) characteristic GC/MS chromatograms of the saturate hydrocarbons of the Agia Zoni II source oil (a) and of oil patches spanning the first 85 days of the oil spill (b to d). (Right) PAH profiles, as relative abundances to the sum of the determined PAH compounds ( $\sum PAH_{32}$ ), of Naph, DBT, Phe, Flth-Pyr and BaA-Chry and their alkyl homologues in the Agia Zoni II source oil (a), average values in oil patches spanning the first 85 days of the oil spill (blue bars) and average values in seawater samples for the corresponding time intervals (red bars) (b to d). For PAH abbreviations see Fig. 2. (For interpretation of the references to color in this figure legend, the reader is referred to the web version of this article.)



determination of total aliphatic hydrocarbons (TAHC) and  $\Sigma\text{PAH}_{32}$  along with the corresponding time series data for the sampling stations S7, S8, S11, S13, S16 and S43 belonging to the Saronikos Gulf systematic monitoring network are summarized in Table S.3. TAHC concentrations ranged from 22.9 to 1220  $\mu\text{g g}^{-1}$ , with an average of 193  $\mu\text{g g}^{-1}$ , showing a SE/NW increasing trend in all samplings with the highest concentrations being recorded at station S7 in Psittaleia Isl. (Fig. 4a). Considering the stations of the Saronikos Gulf systematic monitoring network, TAHC concentrations after the incident varied at lower levels in almost all cases (Table S.3). A similar distribution was also observed for the  $\Sigma\text{PAH}_{32}$  concentrations which ranged from 53.1 to 4570  $\text{ng g}^{-1}$ , with an average of 1180  $\text{ng g}^{-1}$  (Fig. 4b) being lower after the incident at S7 station in Psittaleia, higher at stations S11 and S13, while in all other cases mixed trends were recorded (Table S.3).

A typical GC trace of the aliphatic fraction of the considered sediment samples is illustrated in Fig. 4c. It is characterized by an elevated UCM/RC ratio, > than 7.7 (average being 11.7) in all but two cases (5.2 and 5.6) – data not presented –. RC compounds were identified as being  $\text{C}_{27}\text{--}\text{C}_{35}$  hopanes, exhibiting a dominant thermodynamically stable 17 $\alpha$ (H), 21 $\beta$ (H)-configuration, with the 17 $\beta$ (H), 21 $\alpha$ (H)-compounds being less prominent, while extended  $\text{C}_{31}\text{--}\text{C}_{35}$  homologues were present as pairs of the  $\text{C}_{22}$  diastereoisomers (22S and 22R) with a 22S/22S + 22R ratio value close to 0.6. The above indicate oil-derived inputs and chronic pollution in the sediments (Brassell and

Eglinton, 1980; Mackenzie, 1984; Wang et al., 1999) which typify the chronic anthropogenic petroleum burden of the Saronikos Gulf, especially in the NW part of the study area (Salamina Isl. and near Piraeus port) as earlier reported (Botsou and Hatzianestis, 2012; H.C.M.R., 2016, 2017; Hatzianestis et al., 2004; Kapsimalis et al., 2014; Sklivagou et al., 2008).

Interestingly, on day 11 from the oil spill incident elevated relative abundances of oil-derived PAHs in respect to  $\Sigma\text{PAH}_{32}$ , ranging from 25.6% to 50.2%, were recorded at stations AZII (nearby the shipwreck), OS3 (offshore of Batis), OS4 (offshore of Elliniko) and OS6 (offshore of Glyfada) (Fig. 1) where the main mass of the spill had reached. However, these values rapidly declined in the following two months and furthermore four months after the incident to values around the average of the whole dataset (~14%; Table 2), followed by a corresponding increase of the relative abundance of pyrolytic compounds in respect to  $\Sigma\text{PAH}_{32}$ . In marine sediments, the predominance of pyrolytic PAHs is common due to their greater stability. PAHs deriving from pyrolytic/combustion sources are strongly associated with fine combustion particles (soot and/or char black carbon) that protect them from degradation in sediments (Simo et al., 1997; Yunker et al., 2002). In contrast, several studies have highlighted the selective degradation of low molecular weight labile compounds such as phenanthrene and its methyl derivatives in the marine environment (Bouloubassi et al., 2012; Parinos et al., 2013b; Simo et al., 1997; Theodosi et al., 2013; Wang et al.,

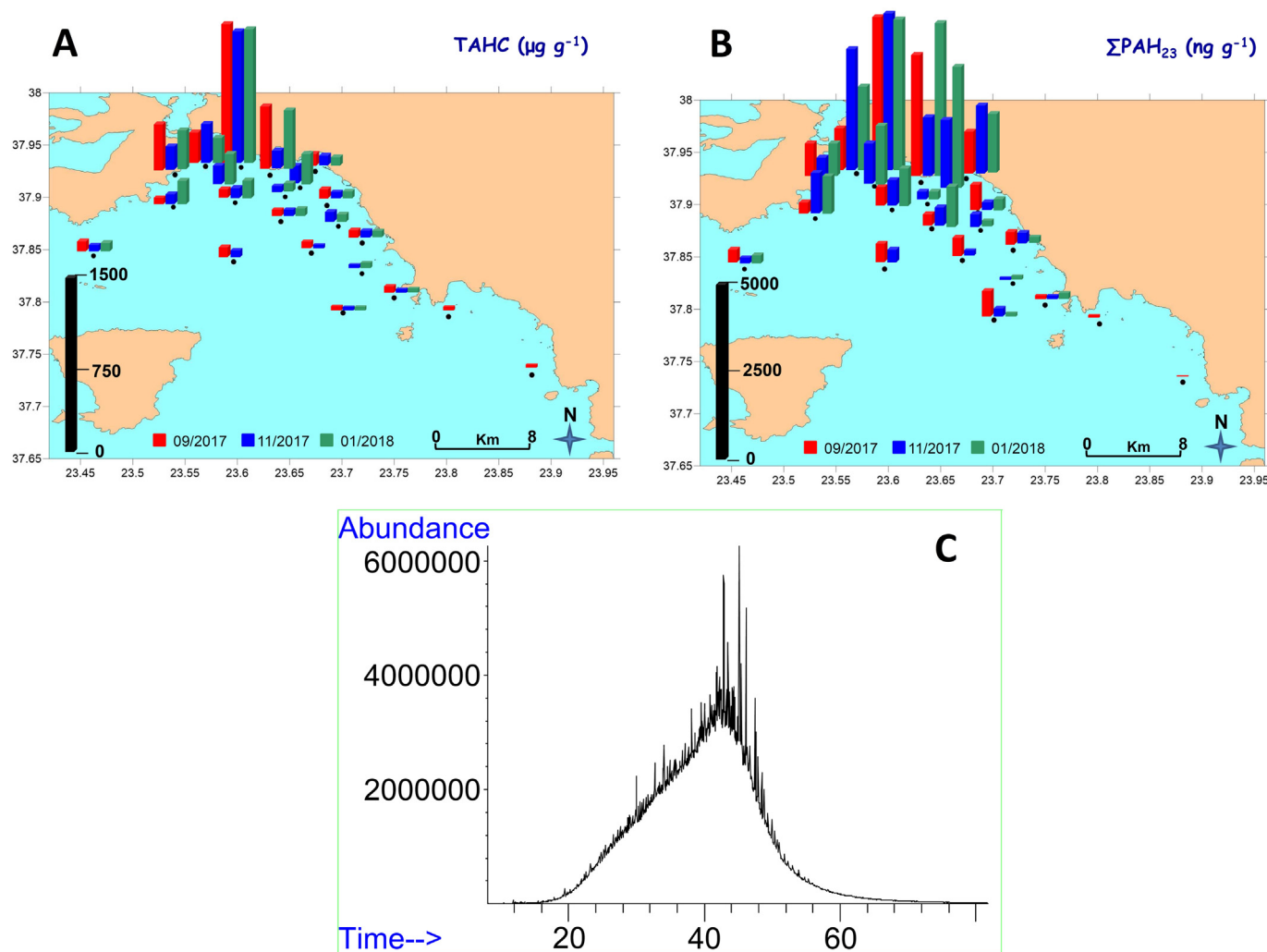


**Fig. 4.** Concentrations of TAHC (in  $\mu\text{g g}^{-1}$ ) (A) and  $\Sigma\text{PAH}_{32}$  (in  $\text{ng g}^{-1}$ ) (B) in the sediments collected in September 2017 (red bars), November 2017 (blue bars) and January 2018 (green bars) in the open Saronikos Gulf, as well as a typical GC trace of the sediment aliphatic fraction (C). (For interpretation of the references to color in this figure legend, the reader is referred to the web version of this article.)



**Table 2**

The percentage distributions of the concentrations of the determined PAHs of pyrolytic origin (sum of compounds with a molecular weight of 202, 228, 252, 276 and 278) and oil-derived compounds (phenanthrene and its methylated derivatives) to  $\sum \text{PAH}_{32}$  for the considered sediment samples.

| Station | Polycyclic aromatic hydrocarbons        |               |              |                                       |               |              |
|---------|---|---------------|--------------|---------------------------------------|---------------|--------------|
|         | Oil-derived (% $\sum \text{PAH}_{32}$ ) |               |              | Pyrolytic (% $\sum \text{PAH}_{32}$ ) |               |              |
|         | September 2017                          | November 2017 | January 2018 | September 2017                        | November 2017 | January 2018 |
| S7      | 12.6                                    | 10.8          | 10.1         | 56.1                                  | 61.5          | 61.6         |
| S8      | 14.1                                    | 12.9          | 11.3         | 58.9                                  | 63.8          | 63.0         |
| S11     | 19.4                                    | 12.7          | 17.6         | 56.5                                  | 65.8          | 56.9         |
| S13     | 11.1                                    | 15.9          | 14.3         | 65.5                                  | 55.1          | 57.3         |
| S16     | 12.4                                    | 13.3          | 14.3         | 67.5                                  | 59.5          | 62.5         |
| S43     | 12.8                                    | 12.7          | 12.1         | 62.9                                  | 64.0          | 63.9         |
| AZ II   | 25.6                                    | 19.0          | 13.2         | 41.3                                  | 51.0          | 61.8         |
| OS1     | 15.2                                    | 12.5          | 11.8         | 55.9                                  | 59.5          | 60.7         |
| OS2     | 12.1                                    | 12.2          | 11.9         | 61.6                                  | 62.7          | 62.3         |
| OS3     | 50.2                                    | 10.1          | 8.9          | 17.4                                  | 67.6          | 69.6         |
| OS4     | 46.6                                    | 17.7          | 14.7         | 22.9                                  | 53.2          | 56.8         |
| OS5     | 20.3                                    | 18.4          | –            | 45.8                                  | 47.2          | –            |
| OS6     | 48.7                                    | 21.2          | 17.9         | 19.6                                  | 42.1          | 59.6         |
| OS7     | 14.7                                    | 11.9          | –            | 55.9                                  | 61.4          | –            |
| OS8     | 16.2                                    | 19.2          | 17.6         | 60.7                                  | 46.6          | 59.2         |
| OS9     | 18.4                                    | –             | –            | 52.7                                  | –             | –            |
| OS10    | 20.3                                    | –             | –            | 56.5                                  | –             | –            |
| OS11    | –                                       | 14.0          | 13.1         | –                                     | 60.1          | 62.1         |
| OS12    | –                                       | 11.8          | 14.7         | –                                     | 65.7          | 55.8         |
| OS13    | –                                       | 14.0          | 15.9         | –                                     | 58.3          | 53.2         |
| OS14    | –                                       | 10.5          | 9.5          | –                                     | 62.9          | 62.8         |
| OS15    | –                                       | 15.7          | 16.2         | –                                     | 59.2          | 54.8         |

1999). Thus, the elevated rates of oil-derived PAHs in the early days of the incident at the abovementioned stations most likely suggest a recent oil pollution imprint.

Indeed, the previous interpretation was confirmed by the GC/MS ion analysis ( $m/z$  71) of the aliphatic fraction for the corresponding sediment samples where an increase in the occurrence of normal alkanes in the  $n\text{-C}_{17}$  to  $n\text{-C}_{26}$  range was observed (Fig. 5). The same molecular profile was evident in the oil patches collected from the coastal zone of the Saronikos Gulf during the early days of the oil spill, as well as in

the molecular profile of the source oil drawn from the wreck (see Fig. 3b and discussion above). The above observations provide good evidence in order to link the identified petroleum imprint with the recent incident of the sinking of the Agia Zoni II. Although it should be considered that heavy oil spills often originate a patchy contamination when sinking offshore which is more difficult to evidence (Franco et al., 2006; Tronczyńska et al., 2004), the presented results support the fact that in all cases this recent burden is mild compared to the high chronic petroleum-associated anthropogenic background of Saronikos Gulf. Actually, this mild recent imprint is not clearly visible in full scan chromatographic analysis of the aliphatic fractions. In the months following the incident (November 2017 and January 2018) this petroleum imprint, following the trend observed for PAH compounds, is reduced to a point that it is not clearly detectable even at the  $m/z$  71 ion analysis. This most likely occurred due to the degradation of the labile oil-derived compounds (aliphatic along with PAHs as discussed above) during their residence in the sediments.

#### 4. Conclusions

This work presents, to the best of our knowledge, the very first investigation of the Agia Zoni II oil spill incident in the Inner Saronikos Gulf, focusing on the evaluation of the spatial and temporal imprint of the spilled oil and deciphering major mechanisms that affected its short-term fate that should be of interest for future scientific research on this and HFO spills in general. The main mass of the Agia Zoni II spilled oil was rapidly beached during the early days after the incident within a rather restricted geographical area, i.e., along 4 km of shoreline on the Salamina Island and along the shorelines on the Elliniko and Glyfada regions. This caused on the one hand an extended petroleum imprint therein but on the other hand allowed the efficient accomplishment of clean-up operations which resulted in reaching background levels of contamination within a period of three months. In the first 85 days of the incident the spilled oil was affected by a combination of volatilization, rapid biodegradation, and photodegradation, most likely attributed to the warm and sunny climatic conditions experienced during this period. Concerning the seabed, an oil imprint was recorded in a few cases being nevertheless mild compared to the chronic petroleum-

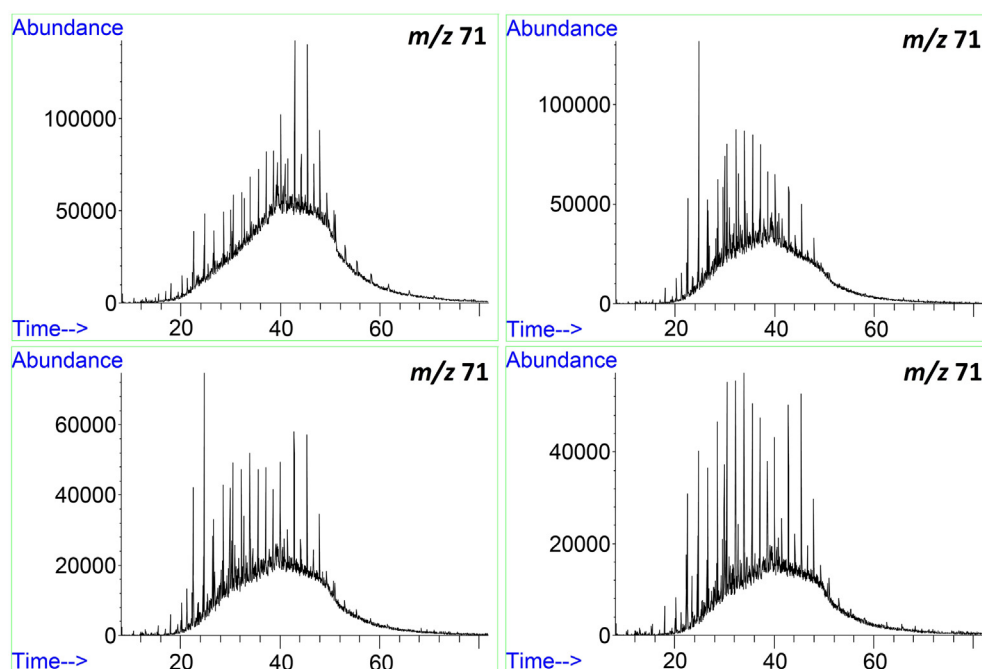


**Fig. 5.** GC/MS trace ( $m/z$  71) of the aliphatic fraction of the collected sediments in September 2017 at stations AZII (nearby the shipwreck; upper left), OS3 (offshore of Batis; upper right), OS4 (offshore of Elliniko; down left) and OS6 (offshore of Glyfada; down right).

associated anthropogenic burden of the Inner Saronikos Gulf, which constitutes the coastal receptor area of the metropolitan city of Athens with approximately four million inhabitants.

## Acknowledgements

This work is part of the monitoring survey performed by the Institute of Oceanography of the Hellenic Centre for Marine Research (H.C.M.R.) after a formal request made by the Hellenic Ministry of Shipping and Island Policy, considering the provisions of paragraphs 3.5.13 and 3.15.1 of the National Emergency Plan on oil pollution incidents (Presidential Decree 11/2002, Government Gazette Issue 6 A'/2002), in order to study the possible short- and medium-term environmental consequences of the incident on the marine ecosystem of Saronikos Gulf. The cost of the monitoring survey was paid for by the International Oil Pollution Compensation Funds (IOPC Funds). We sincerely thank the officers and crew of the R/V Aegaeo (H.C.M.R.) for their precious assistance during cruises, and Vassilis Mpampas and Constantine Fostiropoulos for their patience and help during the conducted coastal samplings. We would also like to thank the two anonymous reviewers for their constructive comments that helped us significantly improve the quality of the current manuscript during the revision process.

## Appendix A. Supplementary data

Supplementary data to this article can be found online at <https://doi.org/10.1016/j.scitotenv.2019.07.374>.

## References

- Arey, J.S., Nelson, R.K., Plata, D.L., Reddy, C.M., 2007. Disentangling oil weathering using GC × GC. 2. Mass transfer calculations. *Environ. Sci. Technol.* 41, 5747–5755.
- Atlas, R.M., 1981. Microbial degradation of petroleum hydrocarbons: an environmental perspective. *Microbiol. Rev.* 45, 180–209.
- Bernabeu, A.M., Fernández-Fernández, S., Bouchette, F., Rey, D., Arcos, A., Bayona, J.M., Albaigés, J., 2013. Recurrent arrival of oil to Galician coast: the final step of the Prestige deep oil spill. *J. Hazard. Mater.* 250–251, 82–90.
- Boehm, P.D., Page, D.S., 2007. Exposure elements in oil spill risk and natural resource damage assessments: a review. *Hum. Ecol. Risk Assess.* 13, 418–448.
- Botsou, F., Hatzianestis, I., 2012. Polycyclic aromatic hydrocarbons (PAHs) in marine sediments of the Hellenic coastal zone, eastern Mediterranean: levels, sources and toxicological significance. *J. Soils Sediments* 12, 265–277.
- Bouloubassi, I., Roussiez, V., Azzoug, M., Lorre, A., 2012. Sources, dispersal pathways and mass budget of sedimentary polycyclic aromatic hydrocarbons (PAH) in the NW Mediterranean margin, Gulf of Lions. *Mar. Chem.* 142, 18–28.
- Brassell, S.C., Eglinton, G., 1980. Environmental chemistry – an interdisciplinary subject. Natural and pollutant organic compounds in contemporary aquatic environments. In: Albaigés, J. (Ed.), *Analytical Techniques in Environmental Chemistry*. Pergamon, Oxford.
- Díez, S., Jover, E., Bayona, J.M., Albaigés, J., 2007. Prestige oil spill. III. Fate of a heavy oil in the marine environment. *Environ. Sci. Technol.* 41, 3075–3082.
- Douglas, G.S., McCarthy, K.J., Dahlen, D.T., Seavey, J.A., Steinhauer, W.G., Prince, R.C., Elmendorf, D.L., 1992. The use of hydrocarbon analyses for environmental assessment and remediation. *J. Soil Contam.* 1, 197–216.
- EC, 2013. Directive 2013/39/EU of the European Parliament and of the Council of 12 August 2013 Amending Directives 2000/60/EC and 2008/105/EC as Regards Priority Substances in the Field of Water Policy.
- Esquinas, N., Rodríguez-Valdés, E., Márquez, G., Gallego, J.L.R., 2017. Diagnostic ratios for the rapid evaluation of natural attenuation of heavy fuel oil pollution along shores. *Chemosphere* 184, 1089–1098.
- Franco, M.A., Viñas, L., Soriano, J.A., de Armas, D., González, J.J., Beiras, R., Salas, N., Bayona, J.M., Albaigés, J., 2006. Spatial distribution and ecotoxicity of petroleum hydrocarbons in sediments from the Galicia continental shelf (NW Spain) after the Prestige oil spill. *Mar. Pollut. Bull.* 53, 260–271.
- González, J.J., Viñas, L., Franco, M.A., Fumega, J., Soriano, J.A., Grueiro, G., Muniategui, S., López-Mahía, P., Prada, D., Bayona, J.M., Alzaga, R., Albaigés, J., 2006. Spatial and temporal distribution of dissolved/dispersed aromatic hydrocarbons in seawater in the area affected by the Prestige oil spill. *Mar. Pollut. Bull.* 53, 250–259.
- Gros, J., Nabi, D., Würz, B., Wick, L.Y., Brussaard, C.P.D., Huisman, J., Van Der Meer, J.R., Reddy, C.M., Arey, J.S., 2014a. First day of an oil spill on the open sea: early mass transfers of hydrocarbons to air and water. *Environ. Sci. Technol.* 48, 9400–9411.
- Gros, J., Reddy, C.M., Aeppli, C., Nelson, R.K., Carmichael, C.A., Arey, J.S., 2014b. Resolving biodegradation patterns of persistent saturated hydrocarbons in weathered oil samples from the Deepwater Horizon disaster. *Environ. Sci. Technol.* 48, 1628–1637.
- Guitart, C., Frickers, P., Horrillo-Caraballo, J., Law, R.J., Readman, J.W., 2008. Characterization of sea surface chemical contamination after shipping accidents. *Environ. Sci. Technol.* 42, 2275–2282.
- H.C.M.R., 2016. Monitoring of the Inner Saronikos Gulf Ecosystem Under the Influence of the Waste Water Treatment Plant of Psittaleia-2nd Period. Scientific Responsible Dr. S. Zervoudaki. Interim Technical Report.
- H.C.M.R., 2017. Monitoring of the Inner Saronikos Gulf Ecosystem Under the Influence of the Waste Water Treatment Plant of Psittaleia-3rd Period. Scientific Responsible Dr. S. Zervoudaki. Interim Technical Report.
- H.C.M.R., Parinos, C., Hatzianestis, I., Karageorgis, A.P., Simbora, N., Panayotidis, P., Tsangaris, C., Strogyloudi, E., Salomidi, M., Kanellopoulos, T.D., Issaris, Y., Chourdaki, S., Plakidi, E., Katsiaras, N., Voutsina, E., Bordbar, L., Kikaki, K., Lardi, P., Arvanitakis, G., Papageorgiou, A., Stavrakaki, I., Kouerinis, N., Gerakaris, V., Pappas, G., Mpampas, V., Fostiropoulos, C., 2018. Study of the Short and Medium Term Environmental Consequences of the Sinking of the Agia Zonia II Tanker on the Marine Ecosystem of the Saronikos Gulf. Final Scientific Report, April 2018, 182 p. Submitted as Information Document to the Thirteenth Meeting of the Focal Points of the Regional Marine Pollution Emergency Response Centre for the Mediterranean Sea (REMPEC), Malta, June 2019. Available at: <http://www.rempec.org/rempec.asp?pg=Visit=New&theID=2013>.
- Hatzianestis, I., Sklivagou, E., 2002. Dissolved and suspended polycyclic aromatic hydrocarbons (PAH) in the North Aegean Sea. *Mediterr. Mar. Sci.* 3, 89–98.
- Hatzianestis, I., Rori, N., Sklivagou, E., Rigas, F., 2004. PAH profiles in dated sediment cores from Elefsis bay, Greece. *Fresenius Environ. Bull.* 13, 1253–1257.
- IOPC, 2019. Latest Developments in the Field of Compensation for Ship-Source Pollution Damage. Working Document of the Thirteenth Meeting of the Focal Points of the Regional Marine Pollution Emergency Response Centre for the Mediterranean Sea (REMPEC), Malta, June 2019. Available at: <http://www.rempec.org/rempec.asp?pg=Visit=New&theID=13>.
- Kalabokas, P.D., Hatzianestis, J., Bartzis, J.G., Papagiannakopoulos, P., 2001. Atmospheric concentrations of saturated and aromatic hydrocarbons around a Greek oil refinery. *Atmos. Environ.* 35, 2545–2555.
- Kapsimalis, V., Panagiotopoulos, I.P., Talagani, P., Hatzianestis, I., Kaberi, H., Rousakis, G., Kanellopoulos, T.D., Hatiris, G.A., 2014. Organic contamination of surface sediments in the metropolitan coastal zone of Athens, Greece: sources, degree, and ecological risk. *Mar. Pollut. Bull.* 80, 312–324.
- Kennicutt II, M.C., Sweet, S.T., Fraser, W.R., Culver, M., Stockton, W.L., 1991. Grounding of the Bahia Paraiso at Arthur Harbor, Antarctica. 1. Distribution and fate of oil spill related hydrocarbons. *Environ. Sci. Technol.* 25, 509–518.
- Lagouvardos, K., Kotroni, V., Bezes, A., Koletsis, I., Kopania, T., Lykoudis, S., Mazarakis, N., Papagiannaki, K., Vougioukas, S., 2017. The automatic weather stations NOANN network of the National Observatory of Athens: operation and database. *Geosci. Data J.* 4, 4–16.
- Lemkau, K.L., Peacock, E.E., Nelson, R.K., Ventura, G.T., Kovacs, J.L., Reddy, C.M., 2010. The M/V Cosco Busan spill: source identification and short-term fate. *Mar. Pollut. Bull.* 60, 2123–2129.
- Lemmon, E.W., Goodwin, A.R.H., 2000. Critical properties and vapor pressure equation for alkanes C<sub>n</sub>H<sub>2n</sub> + 2: normal alkanes with n ≤ 36 and isomers for n = 4 through n = 9. *J. Phys. Chem. Ref. Data* 29, 1–39.
- Mackenzie, A.S., 1984. Applications of biological biomarkers in petroleum geochemistry. In: Brooks, J., Welte, D. (Eds.), *Advances in Petroleum Geochemistry*. Academic Press, London, pp. 115–214.
- Neff, J.M., 2002. Bioaccumulation in Marine Organisms. Effect of Contaminants from Oil Well Produced Water. Elsevier, Amsterdam (452pp).
- NRC, 2003. Oil in the Sea III: Inputs, Fates, and Effects. The National Academies Press, Washington DC.
- Panagiotopoulos, I., Kapsimalis, V., Hatzianestis, I., Kanellopoulos, T.D., Kyriakidou, C., 2010. Environmental status of the metropolitan river (Kifissos) of Athens, Greece. *Environ. Earth Sci.* 61, 983–993.
- Parinos, C., Gogou, A., 2016. Suspended particle-associated PAHs in the open eastern Mediterranean Sea: occurrence, sources and processes affecting their distribution patterns. *Mar. Chem.* 180, 42–50.
- Parinos, C., Gogou, A., Bouloubassi, I., Pedrosa-Pàmies, R., Hatzianestis, I., Sanchez-Vidal, A., Rousakis, G., Velaoras, D., Krokos, G., Lykousis, V., 2013a. Occurrence, sources and transport pathways of natural and anthropogenic hydrocarbons in deep-sea sediments of the eastern Mediterranean Sea. *Biogeosciences* 10, 6069–6089.
- Parinos, C., Gogou, A., Bouloubassi, I., Stavrakakis, S., Plakidi, E., Hatzianestis, I., 2013b. Sources and downward fluxes of polycyclic aromatic hydrocarbons in the open southwestern Black Sea. *Org. Geochem.* 57, 65–75.
- Pavlidou, A., Kontoyiannis, H., Zarokanelos, N., Hatzianestis, I., Assimakopoulou, G., Psyllidou-Giouranovits, R., 2014. Seasonal and Spatial Nutrient Dynamics in Saronikos Gulf: The Impact of Sewage Effluents From Athens Sewage Treatment Plant, Eutrophication: Causes, Consequences and Control. Springer, Netherlands, pp. 111–130.
- Peters, K.E., Walters, C.C., Moldovan, J.M., 2005. Biodegradation Parameters. The Biomarker Guide: Biomarkers and Isotopes in Petroleum Exploration and Earth History. pp. 645–708.
- Plata, D.L., Sharpless, C.M., Reddy, C.M., 2008. Photochemical degradation of polycyclic aromatic hydrocarbons in oil films. *Environ. Sci. Technol.* 42, 2432–2438.
- Radović, J.R., Aeppli, C., Nelson, R.K., Jimenez, N., Reddy, C.M., Bayona, J.M., Albaigés, J., 2014. Assessment of photochemical processes in marine oil spill fingerprinting. *Mar. Pollut. Bull.* 79, 268–277.
- Reddy, C.M., Quinn, J.G., 2001. The North Cape oil spill: hydrocarbons in Rhode Island coastal waters and Point Judith Pond. *Mar. Environ. Res.* 52, 445–461.
- Simo, R., Grimalt, J.O., Albaigés, J., 1997. Loss of unburned-fuel hydrocarbons from combustion aerosols during atmospheric transport. *Environ. Sci. Technol.* 31, 2697–2700.
- Sklivagou, E., Varnavas, S.P., Hatzianestis, I., Kaniias, G., 2008. Assessment of aliphatic and polycyclic aromatic hydrocarbons and trace elements in coastal sediments of the Saronikos Gulf, Greece (Eastern Mediterranean). *Mar. Georesour. Geotechnol.* 26, 372–393.

- Stout, S.A., Wang, Z., 2007. Chemical fingerprinting of spilled or discharged petroleum — methods and factors affecting petroleum fingerprints in the environment. In: Wang, Z., Stout, S.A. (Eds.), *Oil Spill Environmental Forensics*. Academic Press, Burlington, pp. 1–53.
- Tarr, M.A., Zito, P., Overton, E.B., Olson, G.M., Adhikari, P.L., Reddy, C.M., 2016. Weathering of oil spilled in the marine environment. *Oceanography* 29, 126–135.
- Theodosi, C., Parinos, C., Gogou, A., Kokotos, A., Stavrakakis, S., Lykousis, V., Hatzianestis, J., Mihalopoulos, N., 2013. Downward fluxes of elemental carbon, metals and polycyclic aromatic hydrocarbons in settling particles from the deep Ionian Sea (NESTOR site), Eastern Mediterranean. *Biogeosciences* 10, 4449–4464.
- Tronczyńska, J., Munschy, C., Héas-Moisán, K., Guiot, N., Truquet, I., Olivier, N., Men, S., Furaud, A., 2004. Contamination of the Bay of Biscay by polycyclic aromatic hydrocarbons (PAHs) following the T/V “Erika” oil spill. *Aquat. Living Resour.* 17, 243–259.
- Uhler, A.D., Stout, S.A., Douglas, G.S., 2007. Chemical heterogeneity in modern marine residual fuel oils. In: Wang, Z., Stout, S.A. (Eds.), *Oil Spill Environmental Forensics*. Academic Press, Burlington, pp. 327–348.
- UNEP, 1984. *Manual for Measuring Oil and Dissolved/Dispersed Petroleum Hydrocarbons in Marine Waters and on Beaches*. Manuals and Guides, no.13. UNESCO, Paris (35p).
- Vasilakos, C., Levi, N., Maggos, T., Hatzianestis, J., Michopoulos, J., Helmis, C., 2007. Gas-particle concentration and characterization of sources of PAHs in the atmosphere of a suburban area in Athens, Greece. *J. Hazard. Mater.* 140, 45–51.
- Wang, Z., Fingas, M., Page, D.S., 1999. Oil spill identification. *J. Chromatogr. A* 843, 369–411.
- Wang, Z., Yang, C., Fingas, M., Hollebone, B., Hyuk Jae Yim, U., Ryoung Oh, J., 2007. Petroleum biomarker fingerprinting for oil spill characterization and source identification. *Oil Spill Environ. Forensics* 73–146.
- Xenarios, S., Bithas, K., 2009. Valuating the receiving waters of urban wastewater systems through a stakeholder-based approach. *Int. J. Water Resour. Dev.* 25, 123–140.
- Yunker, M.B., Macdonald, R.W., Vingarzan, R., Mitchell, R.H., Goyette, D., Sylvestre, S., 2002. PAHs in the Fraser River basin: a critical appraisal of PAH ratios as indicators of PAH source and composition. *Org. Geochem.* 33, 489–515.